Pillared layered structures *vs.* zeolites as sorbents and catalysts

Part 3.†—Comparison between some alumina-PILCs in ethylbenzene conversions to diethylbenzene and to styrene

Giorgio Perez,[a] **Adriana De Stefanis**[b] **and Anthony A. G. Tomlinson***[b]

[a]*Istituto di Cromatografia, Area della Ricerca di Roma del C.N.R., C.P. 10 Monterotondo Staz., 00016 Roma, Italy*
[b]*Istituto di Chimica dei Materiali, Area della Ricerca di Roma del C.N.R., C.P. 10 Monterotondo Staz., 00016 Roma, Italy*

The pore structures of several alumina-pillared clays (PILCs) have been investigated *via* conversions of ethylbenzene (EB) to diethylbenzenes (DEB) and to styrene (Styr) under Lewis acid conditions. PILCs (including those containing Fe in the pillar) give higher EB→DEB conversion, with a comparable selectivity towards *p*-DEB to that of ZSM-5s ($SiO_2/AlO_2 = 35$, 235) and other mid-pore zeolites. Detailed comparisons of catalytic properties suggest the PILCs contain specific pore exit channels, or dimensions similar to those found in ZSM-5 zeolites, rather than a random supermesh structure. They differ from mid-pore zeolites in acting more as acidic reaction vessels (conversely the shape-selectivity characteristic of ZSM-5s depends on pore access–exit modes). This implies that the alumina pillar controls sorbate molecular orientation during this bimolecular reaction. Zeolites do not give EB→Styr conversion, and the PILCs themselves are active only at $>450\,°C$, and then non-selectively. They become much more active and highly selective (over a wide temperature range: 100–600 °C) only after cation exchange. Beidellitic-PILCs are more active and selective than montmorillonite-PILCs and those containing mixed $Fe^{2+}Fe^{3+}/Al^{3+}$ pillars (*e.g.* FAZA, derived from a Greek bentonite) more than those with unsubstituted alumina pillars. Conversion yields for FAZA lie in the order: $Ni^{2+} > Co^{2+} > Cu^{2+}$, with Ni^{2+}-FAZA the most unfavoured as regards disproportionation (2.5% at 450 °C). Although Cu^{2+}-FAZA gives low conversions of styrene ($<12\%$ at 500 °C) it shows the highest selectivity (100%). The high activity and selectivity for K^+-FAZA suggest that $KFeO_2$ is formed at the alumina pillar, as suggested for commercial α-Fe_2O_3 catalysts. Possible reaction mechanisms and active sites are proposed.

The conversions of ethylbenzene to diethylbenzene, EB→DEB, especially to the more valuable *p*-DEB, and to styrene (Styr) in porous catalysts are still important industrially. Investigations of the former involve mainly mid-pore zeolites,[1] whereas styrene formation by oxidative or non-oxidative dehydrogenation of ethylbenzene feedstock (an industrial process some 60 years old[2]) is feasible (albeit not in industrial use) on a wide variety of oxide and phosphate-based catalysts.[3] In industry, the most frequently used are K^+-promoted Fe_2O_3-based catalysts, variants such as the Shell 015 dehydrogenation catalyst (the Badger process catalyst),[4] and the Dow alkaline-earth-metal NiP catalysts are less widely adopted. Despite improvements in both process and catalyst formulation over the years, low selectivity and migration of potassium ions with loss of activity remain major problems. Hence a recent resurgence of interest in EB dehydrogenation,[5] and attempts to find new catalysts for the reaction, which now include a wider range of materials: from α-Fe_2O_3 dispersions in mid-pore zeolites to carbon molecular sieves.[6]

Concurrently, much effort is directed to understanding the formation, sorption properties and catalytic activity of smectite clays pillared by nano-oxide particles (PILCs).[7] However, although advances in materials preparation are making better-defined solids available, porosity and acidity definition for these materials still constitute problems. The standard BET N_2 method systematically underestimates available internal surface[8] (among other defects) and no agreed acidity scale for solids yet exists.[9] Site selectivity indices, *i.e.* probing surface characteristics of a porous material *via* catalysis, as established many years ago for zeolites, and still being extended,[10] would give a more realistic assessment of the internal surfaces available for reaction, and also allow more quantitative treatment of the considerable sorption and catalysis results available on PILCs, such as those reported by us previously.[11] Comparison with EB→DEB conversion in mid-pore zeolites, traditionally used to assess the *para*-directing capabilities,[12] provides a rough measure of porosity and tortuosity between the two. Secondly, the specific requirements for producing Styr from EB, a reaction not shown by zeolites, should throw light on the nature of the nano-oxide pillar present in PILCs. Catalytic reactions of alumina-PILCs have involved mainly small-molecule transformations (CO, NO_x, syngas conversion, cracking and deep oxidation processes).[13] During extensive catalytic assessment of alumina-pillared clays, several were found to be active in the controlled dehydrogenation of EB to styrene.[14] Particularly high activity was shown by PILCs with iron-containing alumina pillars and we here give details of the reaction and preliminary correlation with the PILC structure.

Experimental

Materials

NH_4^+ forms of ZSM-5 (SiO_2/Al_2O_3 ratios 35 and 235) and BP-PILC (an alumina-pillared montmorillonite) were provided by BP Chemicals (UK) and AZA and FAZA (alumina-pillared zenith bentonites: AZA without, and FAZA with Fe^{2+}/Fe^{3+} in the alumina pillars) by Straton Hi-tec Ltd. (Greece). Al-PILP is an alumina-pillared α-tin phosphate, prepared and characterised as reported elsewhere.[15] Ethylbenzene was a gas-chromatographic standard of purity $>99.95\%$ from C. Erba (Italy). The other chemicals were research grade products, used without further purification.

Cation-exchanged PILCs

Metal-exchanged PILCs and PILPs were prepared as reported previously.[16] In a typical example, FAZA (2.5 g) was ground,

---

† Part 2, A. De Stefanis, G. Perez, O. Ursini and A.A.G. Tomlinson, *Appl. Catal. A: General*, 1995, **132**, 353.

sieved (200 mesh) and dispersed in 500 ml of a 0.1 mol dm^{-3} solution of cobalt(II) acetate. The suspension was heated at 70 °C for 12 h and the exchanged solid filtered off, washed well with deionized water and air-dried. The exchange was repeated three times and the final material dried for 5 h at 50 °C.

Procedures

Both vial and dynamic procedures were used in catalytic testing. In the former, a weighed quantity (3–60 mg) of catalyst in a tared vial was activated at 450 °C for 2 h. Known, excess volumes of ethylbenzene were supplied by syringe, and the vial sealed and heated for varying times. As low temperatures as possible were used (100–200 °C) to avoid coking by pyrolysis products (ethylbenzene gives rise to benzene and ethene on pyrolysis).

Dynamic testing procedures utilised a pyrolyser (SGE Pyrojector II) modified to work as a fixed-bed reactor. The apparatus permits very low amounts of catalyst to be assessed rapidly; operating details and methods for extracting catalytic parameters are given elsewhere.[16] Briefly, low concentrations of reactant with respect to catalyst are used (reducing coking phenomena) and tests with different catalysts at the same WHSV (space velocity) give differing conversion *vs.* time on-stream. Hence, the ratio between product yields from competitive reactions also varies, and extensive testing on standard H^+-ZSM-5 zeolites has demonstrated that the technique provides all the standard catalytic characterisation parameters (temperature, conversion, selectivity, estimates of differences between activation energies of different catalysts). Time on-stream can also be determined, and diffusion is not the rate-determining factor.[16]

Analysis

Effluent products were analysed by GC on a 25 m × 0.32 mm i.d. HP1 column. The amount of the products was measured from the areas of the eluted peaks using appropriate calibration factors. Subsequent identification was carried out on a computer-controlled Hewlett-Packard 5890 gas chromatograph connected to a 5972 mass selective detector.

Results and Discussion

EB→DEB conversion

Table 1 gives the composition of the aromatic fraction for a typical reaction of EB (50 µl) with FAZA in a vial after 17 h at 400 °C. Apart from the major products, benzene and isomeric DEBs, the reaction also gives toluene, styrene, isomeric ethyltoluenes and isopropylbenzene. EB conversion depends linearly on catalyst loading (up to 50 mg of catalyst, at least) whereas in the same loading range the yield in benzene increases faster than that of DEBs (see Fig. 1). Comparison between the plots of Fig. 1 leads to the conclusion that when the mass/mass ratio between catalyst and EB is greater than 1, both benzene formation and EB conversion rates decrease, implying that benzene ethylation occurs. The selectivity towards *para*-isomers (DEB and ET) is higher than expected from thermodynamic equilibrium.[1,3]

Table 1 Composition of the aromatic fraction after reaction of EB over FAZA[a]

	FAZA/mg			
compd (%)	10	20	50	100
B	4.43	7.58	16.12	20.08
T	0.21	0.44	1.67	3.11
EB	91.93	87.35	75.55	64.65
p-X + *m*-X	0.08	0.20	0.17	0.15
Styr	0.15	0.17	0.12	0.14
i-PB	0.04	0.05	0.11	0.12
m-ET		0.05	0.16	0.26
p-ET	0.29	0.45	1.25	0.40
o-ET	0.04	0.09	0.25	2.28
$\sum$ ET	0.33	0.59	1.66	2.94
p-DEB	1.68	2.14	3.52	4.29
m-DEB	1.12	1.23	1.76	2.16
o-DEB	0.22	0.28	0.48	0.73
$\sum$ DEB	3.02	3.66	5.76	7.18

[a] Conditions: 50 µl, 400 °C, 17 h.

At reaction temperatures of 150–250 °C (*i.e.* at very low EB conversion) and varying reaction times (1–4 h), the only detectable products in the aromatic fraction are benzene and DEBs and the measured benzene/DEBs molar ratio now becomes 1. This demonstrates that ethene is not formed, which was confirmed by carrying out dynamic reaction runs (pyrolyser) with FAZA at 200 °C. Since gas-phase protonation of EB leads to benzene and ethene alone,[17] we can conclude that the reaction indeed occurs in the closed PILC environment and also that it involves a bimolecular mechanism. From plots analogous to those in Fig. 1, we calculate the experimental conversion rates to be 0.021, 0.049 and 0.148 at 150, 200 and 250 °C (expressed as % EB converted per mg of FAZA per hour). Fig. 2(*a*) shows EB total conversion yields at 200 °C for all the materials. Clearly, the highest EB conversion and the highest yields in both benzene and DEBs are obtained on BP-PILC, but the other two PILCs, AZA and even more so FAZA, also give rise to appreciable quantities of DEB, and with a more favourable DEB/B ratio than does BP-PILC. Since a bimolecular reaction is involved, blocking of the pores in the PILCs by cation exchange is expected to lead to lower activity, which is indeed the case for all the exchanged FAZA materials. Conversely, we ascribe the low conversion yields for Al-PILP and ZSM-5(235) to the operation of acidity effects alone.

This is the first time (in the absence of detailed X-ray structural information, not extractable from this type of material) that PILCs have been shown to possess a *p*-directing character. The fact that all the PILCs show higher *p*-directing tendency than mid-pore zeolites [see Fig. 2(*b*); the only exception is BP-PILC] is of interest because it indicates that the pillar topology is more ordered than that derived from a supermesh structure (which supposes that although the polyhydroxyoxy cation insertion in the preparation may be ordered,

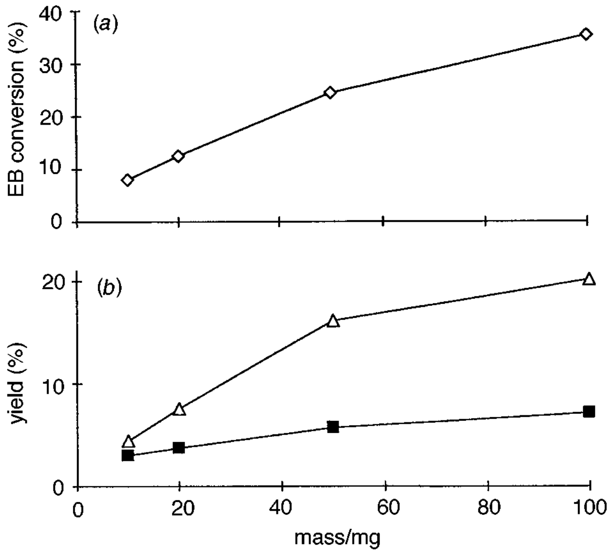

Fig. 1 Influence of catalyst loading on EB→DEB conversion (vial experiments, 400 °C, 17 h). (*a*) Ethylbenzene conversion *vs.* mass of FAZA catalyst loaded; (*b*) yields of benzene (△) and DEB (■) *vs.* mass of FAZA catalyst.

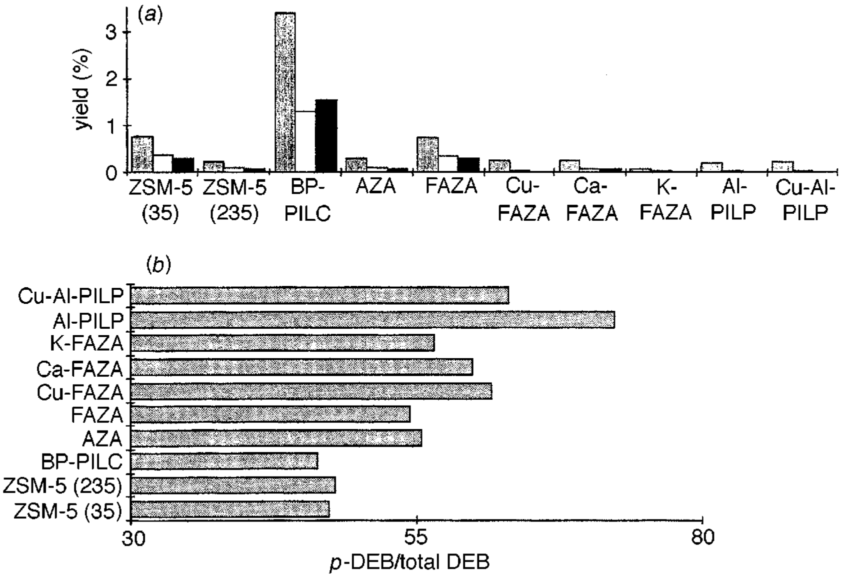

Fig. 2 (*a*) Comparison of EB pyrolysis for the catalysts (conditions: 200 °C, 17 h, 4 ± 0.2 mg) (EB grey, B white, DEB black); (*b*) *p*-selectivity (*p*-DEB/$\sum$ DEB)

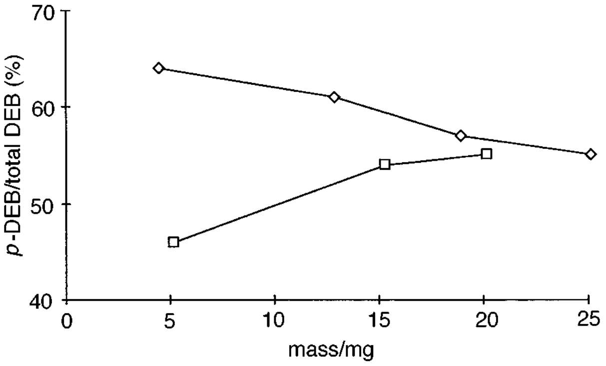

Fig. 3 Comparison of *p*-DEB/total DEB ratios between FAZA (◇) and ZSM-5/35 (□) *vs.* catalyst loading (vial experiment, 200 °C, 4 h)

the calcination step leads to an entirely random distribution of alumina pillars).[18]

Furthermore, inspection of Fig. 3, which compares *para*-selectivity for FAZA and ZSM-5/35 with loading, shows that an increase in catalyst loading generally leads to a decrease in *para*-selectivity for PILCs, but not for ZSM-5s. In other words, the PILC acts more as an acidic catalytic reaction vessel, whereas ZSM-5/35 does not. In agreement with this and with the access channel being more important than the exit channel (in these PILCs, at least)[19] both ZSM-5s show little coking, but FAZA shows much more. This underlines the basic difference between the two classes of porous materials: in PILCs the electrostatic anisotropy between sheet and pillar, which has in some cases been estimated,[20] is the controlling factor in molecular orientation of sorbates, whereas in zeolites it is access–exit to pores.

Following EB→DEB conversion and *p*-DEB/DEBs ratios with temperature brings to light further differences between the PILCs and mid-pore zeolites. On all the zeolites tested, EB undergoes mainly dealkylation on increasing the reaction temperature. The fraction of DEBs in the converted products decreases slightly when USY is used, faster and to about the same extent for both ZSM-5s, and dramatically so with H$^+$-mordenite (Fig. 4). At temperatures >250 °C, only BP-PILC (like USY) maintains appreciable selectivity (*ca.* 46%) for DEBs; under dynamic testing conditions (*i.e.* with a low amount of EB compared to catalyst) all the other PILCs and PILPs give a different spectrum of products. A *para*-selectivity plot for the zeolites leads to the conclusion that H$^+$-mordenite and ZSM-5/35 show a high *para*-directing tendency, which decreases slightly as the temperature decreases [Fig. 4(*b*)]. Instead, USY shows no *p*-direction (*p*-DEB being near the thermodynamic equilibrium value of 31.3 at 200 °C), which confirms the literature data.[21] Again, ZSM-5/235 shows a different tendency: on increasing the temperature its selectivity increases to reach that of the other *para*-directing zeolites.

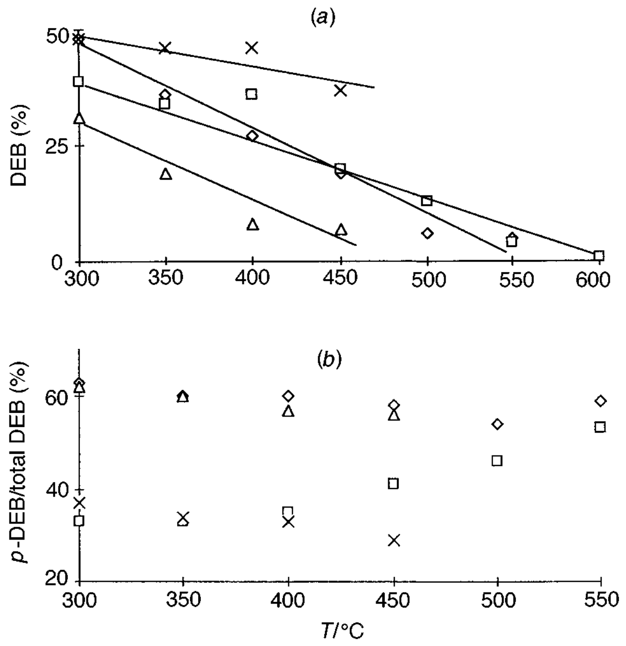

Fig. 4 (*a*) EB→DEB conversion in the compared zeolites with respect to temperature; (*b*) *p*-DEB/total DEB ratios with temperature (ZSM5/35 ◇, ZSM5/235 □, H$^+$-mordenite △, USY ×)

Several points need to be made on mechanisms, which are still not established for mid-pore zeolites. EB→DEB conversion over β-zeolite and ZSM-5 is believed to be governed by the reaction temperature:[22] pore size plays little role in deciding isomer selectivity, but as temperature increases, the number of Brønsted acid sites decreases. Further, the disproportionation reaction is governed by kinetic, rather than thermodynamic, controls at lower temperatures. Other workers have instead found a high *para*-selectivity in ZSM-35,[23] and from experiments carried out by mechanically mixing ZSM-35 and ZSM-5, Rane *et al.* suggested that ZSM-5 is the best catalyst for EB disproportionation itself, whereas ZSM-35 directs the subsequent isomerization to *p*-DEB. We recall that apart from disproportionation, EB also undergoes dealkylation (benzene is formed in excess with respect to DEBs) and side-chain fragmentation (toluene is recovered among the products) in both ZSM-5 and ZSM-35.[24] On wide-pore zeolites a thermodynamic equilibrium mixture of isomers is formed, also suggested to occur in Y zeolite,[25] and (further pursuing this point) by addition of *n*-alkanes, Bhat and Halgery[26] demonstrated that EB conversion indeed occurs inside the zeolite pores.

Now, the reaction mechanism proposed in the literature involves a de-ethylation/ethylation process as the first step, EB being converted into benzene and ethene. The latter undergoes protonation to $C_2H_5^+$, which subsequently adds to the excess of EB present to give DEB. At first sight, this reaction model appears to be confirmed by the absence of DEBs in platinum-exchanged ZSM-35,[27] given that ethane forms readily from ethene in the presence of a hydrogenating centre (Pt^{2+}) which prevents formation of alkylating agent. However, experiments have excluded EB ethylation by $C_2H_5^+$ ions as energetically unfavoured in both classical solution chemistry (where counter ions are formed[28]) and gas-phase chemistry, where carbonium ions are formed[29] (although they are, of course, protonating agents for arenes). The role of $C_2H_5^+$ proposed is therefore dubious and the asymmetric transition-state model suggested by van Santen and co-workers,[30] in which the cation is anchored to the zeolite, is more convincing. We suggest that DEB formation occurs between EB molecules entering into, and EB-derived cations exiting from, the ZSM-5 channels, but cannot yet suggest a reaction site for the PILCs because of ambiguity in the location of the cation (between pillar and sheet).

EB→styrene conversion

Dynamic experimental conditions differ from vial experiments in both the large excess of catalyst with respect to reagent and in reaction time, which is reduced from hours to milliseconds. Among other changes, a decrease in EB conversion would then be expected under these conditions. Comparing the results of Table 1 for FAZA with those under dynamic conditions (Table 2), shows that the latter leads to styrene as major product. The other PILCs have analogous behaviour, although AZA, FAZA, Cu-AZA and Ca-FAZA gave low yields (2–8.5%) as listed in Table 3, which lists styrene yield as a function of reaction temperature at approximately the same catalyst loading. Among the non-PILC catalysts tested, Al-PILP and ZSM-5/235 alone gave styrene, but only in trace amounts (<1%). Selectivities are shown in Fig. 5.

Table 2 EB conversion in FAZA at different temperatures[a]

	300 °C	350 °C	400 °C	450 °C	500 °C
B	0.31	0.58	0.90	1.00	1.09
T	0.01	0.02	0.03	0.03	0.04
EB	98.65	98.59	97.49	95.67	92.40
Styr	0.36	0.68	1.46	3.28	4.33
DEBs	0.03	0.08	0.10	0.09	0.07

[a]Conditions: dynamic runs, 0.2 µl EB, 33.5 mg FAZA.

Mechanisms and active sites

In summary, this is a rare example of a dehydrogenation reaction occurring in PILCs but not in zeolites, the exception (BP-PILC, which is very acidic) underlining the importance of the alumina pillar in directing the reaction. However, it is not the first dehydrogenation reaction to be observed in a PILC: in pulse conditions, cumene undergoes dehydrogenation to give *o*-methylstyrene on silica-pillared rectorite.[31] The yields are comparable to ours but the selectivity is much lower, as seen in the *ca.* 100% selectivity on K-FAZA (Fig. 5). From reaction rates calculated from contact times (Table 4) we deduce that at least four primary reactions occur when EB reacts in PILCs: (1) decomposition of EB to benzene and ethene; (2) transalkylation: 2EB to DEB + benzene; (3) oxidative dehydrogenation: EB to Styr; and (4) ethyl group cracking to give toluene.

Reactions (1) and (4) occur at high temperatures (>450 °C), reaction (2) at high EB concentration with respect to the catalyst (as in vial experiments) and reaction (3) is typical of PILCs; it does not occur with zeolites. The selectivities are particularly striking for Cu^{2+}-exchanged materials and for K^+-FAZA, which yields styrene alone (even at 600 °C) although with a reaction rate lower than in the other PILCs, and rapid deactivation: to 20% activity after 1 h and to <1% after 4 h. The yield curves for styrene production indicate that two mechanisms are probably in operation, and since no product from a bimolecular reaction (*e.g.* biphenyl derivatives) was obtained, the initial mechanism probably involves attachment of a single EB molecule. We conclude that a very specific transition state for EB occurs in PILCs, which is underlined by the fact that bulkier alkylarenes do not undergo oxidative dehydrogenation under the same conditions.

A choice between pillar and sheet attachment of EB in the PILC pore is difficult. Nevertheless, K^+-FAZA ($\leqslant$25% conversion and *ca.* 100% selectivity) provides analogies with the K^+-promotion found in the industrial catalysts. On the basis of Mössbauer results, the iron-alumina pillar in FAZA has recently been assigned a 'pancake' structure of dimensions *ca.* 1×9.5 ($\pm$2.5) nm containing dispersed Fe^{2+} and Fe^{3+}.[32] Suggestively, surface 'islands' of $KFeO_2$ with formation of numerous very small pores have recently been proposed as the active sites in the commercial K^+-α-Fe_2O_3–Al_2O_3 catalysts.[4,5] Given the similar structures involved, we suggest that K^+-exchange in FAZA occurs selectively at the oxide pillar with subsequent formation of $KFeO_2$ on the pancake 'sides' on calcination (see Fig. 6). In addition, we provisionally ascribe the superior selectivities and lower temperatures (400–550 °C) compared with K^+-promoted Fe_2O_3 industrial catalysts to

Table 3 Styrene yields (%) for the catalysts at different temperatures[a]

	250 °C	300 °C	350 °C	400 °C	450 °C	500 °C	550 °C	600 °C
AZA	0.15	0.49		1.31	1.45	2.28	5.3	9.16
FAZA	0.12	0.36	0.68	1.46	3.28	4.33	7.6	
Cu-AZA	0.52		1.17	2.9	5.45	8.18		
Cu-FAZA		3.05	3.66	4.31	8.08	12.6		
Cu-Al-PILP	1.68	4.85	11.51	19.25	23.63	14.45	12.2	
Ca-FAZA	0.13	0.66	1.7	3.16	4.17	5.19		
K-FAZA	0.11	0.5	1.28	2.78	7.7	9.97	13.2	
Co-FAZA		1.09		3.29	7.99	11.04	16.46	22.8
Ni-FAZA	0.47	1.35	2.69	5.12	14.82	25.4	29.3	34.61

[a]Conditions: 0.2 µl EB + 33.5 ± 0.4 mg catalyst.

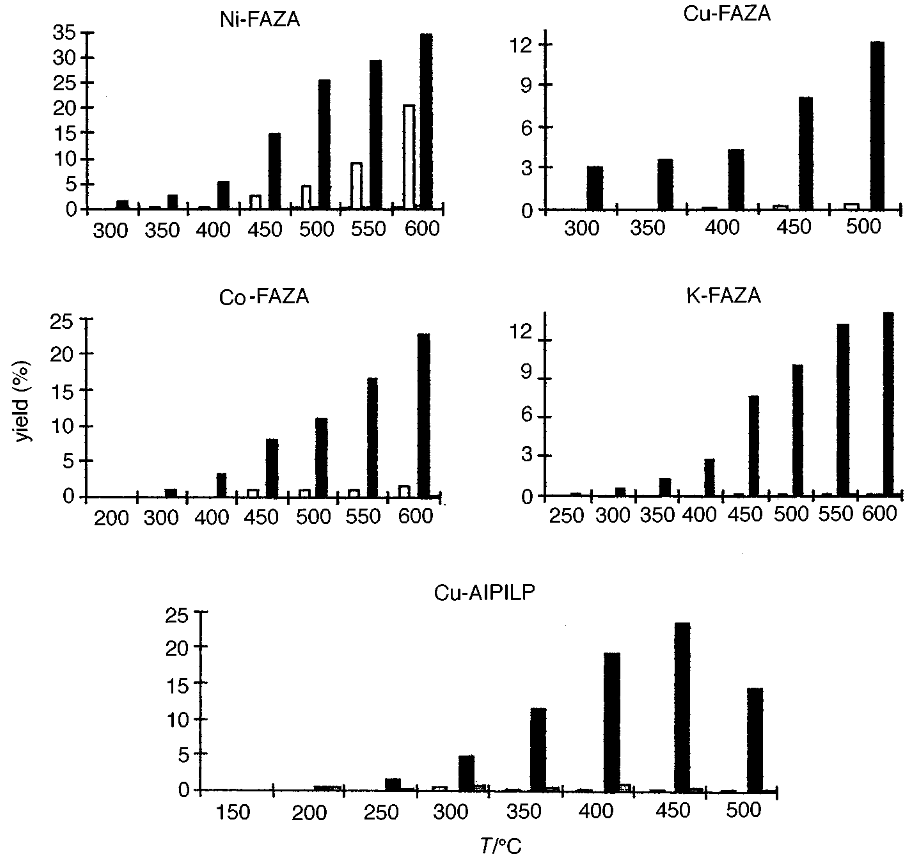

Fig. 5 EB→styrene conversion on some metal-exchanged FAZAs and Cu-Al-PILP (B ☐, Sty ■)

Table 4 Reaction rates[a] calculated for 0.1 μl of EB at different temperatures

	490 °C	510 °C	530 °C	550 °C	570 °C
Cu-FAZA		9.9	12.3	16.8	25.4
K-Cu-FAZA	5.2	8.4	15.0	21.1	30.6
Ni-FAZA	18.2	25.8	35.0	48.9	64.6
Ca-Cu-FAZA	3.6	4.1	4.8	8.6	10.3
K-FAZA	8.7	12.9	18.8	23.7	36.2

[a] nmol (mg of catalyst)$^{-1}$ ns^{-1} × 10^{-2}.

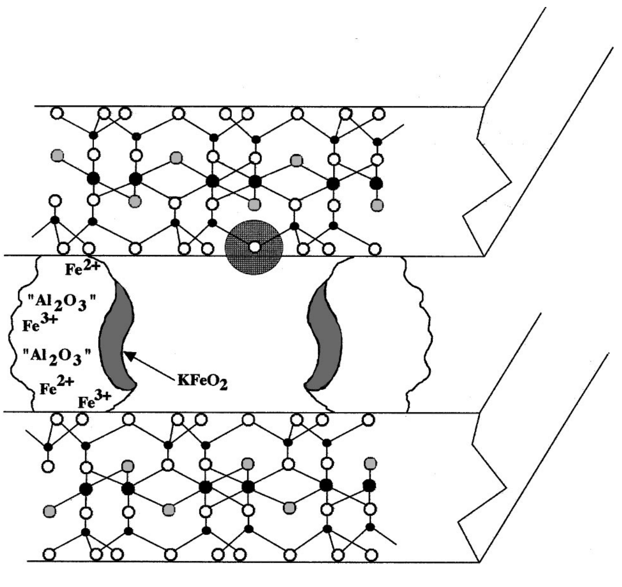

Fig. 6 Possible active site in K^+-exchanged FAZA. K^+ ions exchanged in layer (grey) may also be present.

more secure anchoring of the K^+ ions in K-FAZA, the pillar being in a restricted environment.

Turning to transition-metal ion active sites, Cu—O—Fe ones may arise from Cu^{2+} bonded either to smectite layers or to Fe-alumina pillars [Cu^{2+} exchange in alumina-PILCs occurs at the pillar, presumably through in-plane coordination of a $Cu(OH_2)_4{}^{2+}$ moiety[33]]. Whichever is the case, Lewis-acid conditions would give rise to low Cu^{2+}-coordination number (well documented for zeolites), a strained interlayer environment and high labilisation tendency of axial Cu^{2+} positions, leading to an unusual cation intermediate bridging the Cu^{2+} and the pillar. Conversely, Co^{2+} and Ni^{2+} activity probably arises *via* four- and five-coordination sites. Finally, the drop in activity for Cu-Al-PILP at >450 °C (see Fig. 5) may be ascribed to layer collapse of the material.

Detailed spectroscopic support for these suggestions is being sought and modelling techniques being utilised to clarify the geometries of the active sites suggested.

Conclusions

From detailed comparisons with mid-pore zeolites, it has been found that alumina-pillared smectite clays and group 14 phosphates have *p*-directing properties in the EB→DEB conversion. Further, after cation exchange, the same PILCs and PILPs are good catalysts for the oxidative dehydrogenation of ethylbenzene to styrene. Both divalent transition-metals ions (Co^{2+}, Ni^{2+}, Cu^{2+}) and non-transition-metal ions (K^+, Ca^{2+}) are active, and the reaction occurs at lower temperatures and with higher selectivity than for the α-Fe_2O_3-based catalysts in industrial use. The most active are Ni^{2+}-zenith-N bentonite PILCs, but the most selective (100% selectivity at 350 °C) are those based on Cu^{2+}- and K^+-exchanged congeners. Different active centres appear to be involved and it is suggested that for K^+-FAZA the active site may contain $KFeO_2$, as for the commercial α-Fe_2O_3 catalysts.

We gratefully acknowledge the BRITE-EuRam programme of the E. U. (contract no. BRE2-CT93-0450) for financial support and Dr. M. P. Atkins of BP Chemicals for generous gifts of BP-PILC and zeolites and for his continuing encouragement.

References

1 W. W. Kaeding, *Catal. Rev.*, 1973, **8**, 307.

2 E. H. Lee, *Catal. Rev.*, 1973, **8**, 285.

3 W. Ruppert, G. Emig and H. Hofmann, *Chem. Z.*, 1983, **107**, 211; G. E. Vrieland, *J. Catal.*, 1988, **111**, 14; Y. Murakami, K. Iwayame, H. Uchida, T. Hattori and T. Tagawa, *J. Catal.*, 1981, **71**, 257; T. Hattori, H. Hanai and Y. Murakami, *J. Catal.*, 1979, **56**, 294.

4 H. H. Al-Marishad and M. V. Lamb, *Hydrocarbon Processing*, 1991, **8**, 125.

5 B. K. Abdallah, S. S. E. H. Elnashaie, S. S. Alkhowaiter and S. S. Elshishini, *Appl. Catal. A*, 1994, **113**, 89; Z. Gao, B. Zhang and J. Cui, *Appl. Catal. A*, 1991, **72**, 331; W. P. Addiego, C. A. Estrada, D. W. Goodman, M. P. Rosynek and R. G. Windham, *J. Catal.*, 1994, **146**, 407, and references therein; F. Tiscareno-Lechuga, C. G. Hill and M. A. Anderson, *Appl. Catal. A*, 1993, **96**, 33.

6 D. W. Lewis, C. R. A. Catlow, G. Sankar and S. W. Carr, *J. Phys. Chem.*, 1995, **99**, 2377; R. S. Drago and K. Jurczyk, *Appl. Catal. A*, 1994, **112**, 117.

7 *Pillared Layered Structures. Current Trends and Applications*, ed. I. V. Mitchell, Elsevier Applied Science, London, 1990; *Expanded Clays and other Mesoporous Materials*, ed. M. L. Occelli and H. A. Robson, Van Nostrand, New York, 1992.

8 J. Bonnardet, J. Fraissard, K. Unger, D. Kim, M. Ferrero, J. Ragle and W. C. Connor, *Stud. Surf. Sci. Catal.*, 1994, **87**, 319.

9 W. Farneth and R. J. Gorte, *Chem. Rev.*, 1995, **95**, 615.

10 W. Souverijns, W. Verrelst, G. Vanbutsele, J. A. Martens and P. A. Jacobs, *J. Chem. Soc., Chem. Commun.*, 1994, 1671.

11 A. De Stefanis, G. Perez and A. A. G. Tomlinson, *J. Mater. Chem.*, 1994, **4**, 959.

12 W. W. Kaeding, C. Chu, L. B. Young, B. Weisnstein and S. A. Buttur, *J. Catal.*, 1981, **67**, 159; W. W. Kaeding, *J. Catal.*, 1985, **95**, 512.

13 *E.g.* J. Barrault, L. Gatineau, N. Hassam and F. Bergaya, *Energy Fuels*, 1992, **6**, 760; M. L. Occelli, J. M. Stencel and S. L. Suib, *J. Mol. Catal.*, 1991, **64**, 221.

14 A. De Stefanis, G. Perez and A. A. G. Tomlinson, *Eur. Pat. Application*, February, 1995.

15 M. A. Maireles-Torres, P. Olivera-Pastor, E. Rodriguez-Castellon, A. Jimenez-Lopez, L. Alagna and A. A. G. Tomlinson, *J. Mater. Chem.*, 1991, **1**, 319.

16 G. Perez, M. R. Raimondo, A. De Stefanis and A. A. G. Tomlinson, *J. Anal. Appl. Pyrol.*, 1995, **35**, 157.

17 E. Lilla and G. Perez, *J. Phys. Chem.*, 1980, **84**, 1306.

18 A. Habti, D. Kernis, P. Levitz and H. Van Damme, *J. Chem. Soc., Faraday Trans. 2*, 1984, **80**, 67; F. Bergaya, L. Gatineau and H. Van Damme, in *Mesoporous Multifunctional Inorganic Solids*, ed. C. A. C. Sequeira and M. J. Hudson, NATO ASI Ser. vol. 400, 1993, p. 19.

19 S. M. Csicsery, in *Zeolites Chemistry and Catalysis*, ed. J. Rabo, ACS Monograph 171, 1976, ch. 12.

20 M. S. A. Baksh and R. T. Yang, *Am. Inst. Chem. Eng. J.*, 1992, **38**, 1357.

21 N. P. Rhodes and R. Rudham, *J. Chem. Soc., Faraday Trans.*, 1993, **89**, 2551.

22 L. Forni, S. Amarilli, G. Bellussi, C. Perego and A. Carati, *Appl. Catal. A*, 1993, **103** 173.

23 S. J. Rane, C. V. V. Satyanarayana and D. K. Chakrabarty, *Appl. Catal.*, 1991, **69**, 77.

24 J. Engelhardt, *J. Catal.*, 1994, **35**, 574.

25 H. G. Karge, Z. Sarbak, K. Hatada, J. Weitcamp and P. A. Jacobs, *J. Catal.*, 1983, **82**, 236; D. S. Santilli, *J. Catal.*, 1986, **99**, 327; N. P. Rhodes and R. Rudham, *J. Chem. Soc., Faraday Trans.*, 1993, **89**, 2551.

26 Y. S. Bhat and A. B. Halgery, *Appl. Catal. A*, 1993, **101**, 95.

27 M. H. W. Burgers and H. van Bekkum, *J. Catal.*, 1994, **148**, 684.

28 D. M. Brower, E. L. Mackor and C. MacLean, in *Carbonium Ions*, ed. G. A. Olah and P. von R. Schleyer, Wiley-Interscience, New York, 1970, vol. 2, p. 864.

29 R. Waldez and J. L. Franklin, *Int. J. Mass Spectrom. Ion Phys.*, 1980, **36**, 85.

30 R. A. van Santen and G. J. Kramer, *Chem. Rev.*, 1995, **95**, 637; V. B. Kazansky, I. N. Senchenya, M. Frash and R. A. Van Santen, *Catal. Lett.*, 1994, **27**, 345.

31 M. L. Occelli, in *Expanded Clays and other Mesoporous Materials*, ed. M. L. Occelli and H. A. Robson, Van Nostrand, New York, 1992.

32 Th. Backas, *Clays Clay Miner.*, 1996, in press.

33 *E.g.* J-M. Comets and L. Kevan, *J. Phys. Chem.*, 1993, **97**, 12004.

Paper 6/04369K; *Received* 24*th June*, 1996